AFRL-AFOSR-VA-TR-2018-0364

An integrated experimental and theoretical exploration of radiation reaction

Douglass Schumacher
OHIO STATE UNIVERSITY THE

01/17/2018
Final Report

Air Force Research Laboratory
AF Office Of Scientific Research (AFOSR)/ RTB1
Arlington, Virginia 22203
Air Force Materiel Command

REPORT DOCUMENTATION PAGE

Form Approved
OMB No. 0704-0188

1. REPORT DATE *(DD-MM-YYYY)*	2. REPORT TYPE	3. DATES COVERED *(From - To)*
12/29/2017	Final Report	04/01/2014 - 03/31/2017

4. TITLE AND SUBTITLE
An integrated experimental and theoretical exploration of radiation reaction, light-sail acceleration, and approaches to the Schwinger intensity limit.

5a. CONTRACT NUMBER

5b. GRANT NUMBER
FA9550-14-1-0085

5c. PROGRAM ELEMENT NUMBER

6. AUTHOR(S)
Schumacher, Douglass W.
Akli, Kramer U.

5d. PROJECT NUMBER

5e. TASK NUMBER

5f. WORK UNIT NUMBER

7. PERFORMING ORGANIZATION NAME(S) AND ADDRESS(ES)
The Ohio State University
1960 Kenny Road
Columbus, OH 43210-1016

8. PERFORMING ORGANIZATION REPORT NUMBER

9. SPONSORING/MONITORING AGENCY NAME(S) AND ADDRESS(ES)
Air Force Office of Scientific Research
875 North Randolph Street, STE 325, Room 3112
Arlington, VA 22203

10. SPONSOR/MONITOR'S ACRONYM(S)
AFOSR

11. SPONSOR/MONITOR'S REPORT NUMBER(S)

12. DISTRIBUTION/AVAILABILITY STATEMENT
Distribution A - Approved for Public Release

13. SUPPLEMENTARY NOTES

14. ABSTRACT
We have performed an extended study of extreme light-plasma interactions. This effort included three thrusts: (1) Identification of signatures of the radiation reaction (RR) and other extreme light effects that might be observed at intensities within an order of magnitude or two of current capability, and thus in the near future; (2) Development of novel target designs that facilitate such experiments; and (3) Experiments to validate the new target designs.

15. SUBJECT TERMS
Laser-plasma interaction, relativistic, radiation reaction, structured target, particle-in-cell simulation, PIC

16. SECURITY CLASSIFICATION OF:			17. LIMITATION OF ABSTRACT	18. NUMBER OF PAGES	19a. NAME OF RESPONSIBLE PERSON
a. REPORT	b. ABSTRACT	c. THIS PAGE			Douglass Schumacher
U	U	U	UU	14	19b. TELEPHONE NUMBER *(Include area code)* 614-292-7035

INSTRUCTIONS FOR COMPLETING SF 298

1. REPORT DATE. Full publication date, including day, month, if available. Must cite at least the year and be Year 2000 compliant, e.g. 30-06-1998; xx-06-1998; xx-xx-1998.

2. REPORT TYPE. State the type of report, such as final, technical, interim, memorandum, master's thesis, progress, quarterly, research, special, group study, etc.

3. DATE COVERED. Indicate the time during which the work was performed and the report was written, e.g., Jun 1997 - Jun 1998; 1-10 Jun 1996; May - Nov 1998; Nov 1998.

4. TITLE. Enter title and subtitle with volume number and part number, if applicable. On classified documents, enter the title classification in parentheses.

5a. CONTRACT NUMBER. Enter all contract numbers as they appear in the report, e.g. F33315-86-C-5169.

5b. GRANT NUMBER. Enter all grant numbers as they appear in the report. e.g. AFOSR-82-1234.

5c. PROGRAM ELEMENT NUMBER. Enter all program element numbers as they appear in the report, e.g. 61101A.

5e. TASK NUMBER. Enter all task numbers as they appear in the report, e.g. 05; RF0330201; T4112.

5f. WORK UNIT NUMBER. Enter all work unit numbers as they appear in the report, e.g. 001; AFAPL30480105.

6. AUTHOR(S). Enter name(s) of person(s) responsible for writing the report, performing the research, or credited with the content of the report. The form of entry is the last name, first name, middle initial, and additional qualifiers separated by commas, e.g. Smith, Richard, J, Jr.

7. PERFORMING ORGANIZATION NAME(S) AND ADDRESS(ES). Self-explanatory.

8. PERFORMING ORGANIZATION REPORT NUMBER. Enter all unique alphanumeric report numbers assigned by the performing organization, e.g. BRL-1234; AFWL-TR-85-4017-Vol-21-PT-2.

9. SPONSORING/MONITORING AGENCY NAME(S) AND ADDRESS(ES). Enter the name and address of the organization(s) financially responsible for and monitoring the work.

10. SPONSOR/MONITOR'S ACRONYM(S). Enter, if available, e.g. BRL, ARDEC, NADC.

11. SPONSOR/MONITOR'S REPORT NUMBER(S). Enter report number as assigned by the sponsoring/ monitoring agency, if available, e.g. BRL-TR-829; -215.

12. DISTRIBUTION/AVAILABILITY STATEMENT. Use agency-mandated availability statements to indicate the public availability or distribution limitations of the report. If additional limitations/ restrictions or special markings are indicated, follow agency authorization procedures, e.g. RD/FRD, PROPIN, ITAR, etc. Include copyright information.

13. SUPPLEMENTARY NOTES. Enter information not included elsewhere such as: prepared in cooperation with; translation of; report supersedes; old edition number, etc.

14. ABSTRACT. A brief (approximately 200 words) factual summary of the most significant information.

15. SUBJECT TERMS. Key words or phrases identifying major concepts in the report.

16. SECURITY CLASSIFICATION. Enter security classification in accordance with security classification regulations, e.g. U, C, S, etc. If this form contains classified information, stamp classification level on the top and bottom of this page.

17. LIMITATION OF ABSTRACT. This block must be completed to assign a distribution limitation to the abstract. Enter UU (Unclassified Unlimited) or SAR (Same as Report). An entry in this block is necessary if the abstract is to be limited.

FINAL PERFORMANCE REPORT FOR AWARD FA9550-14-1-0085 (BRI)

Primary Contact E-mail: *Schumacher.60@*osu.edu

Primary Contact Phone Number: 614-292-*7035*

Institution name: The Ohio State University

Title: An integrated experimental and theoretical exploration of radiation reaction, light-sail acceleration, and approaches to the Schwinger intensity limit.

AFOSR assigned control number: FA9550-14-1-0085

Principal Investigator Name: Douglass Schumacher.
K. U. Akli was PI for the first two years.

Program Manager: Dr. Enrique Parra

Reporting Period Start Date: 04/01/2014

Reporting Period End Date: 03/31/2017

Abstract

We have performed an extended study of extreme light-plasma interactions. This effort included three thrusts: (1) Identification of signatures of the radiation reaction (RR) and other extreme light effects that might be observed at intensities within an order of magnitude or two of current capability, and thus in the near future; (2) Development of novel target designs that facilitate such experiments; and (3) Experiments to validate the new target designs. RR effects occur when the field radiated by an electron modifies the motion of the electron itself, and they can be significant for extreme relativistic intensities exceeding 10^{22} W/cm^2. We have shown using particle-in-cell (PIC) simulations that include a quantum electrodynamics model for treating the radiation reaction and γ-ray emission that above a threshold intensity, significant RR occurs that traps a large population of electrons within the laser pulse. One result is strong γ-ray emission that could be used as a measurement of the RR effect itself. We have explored this effect, the resulting energy partition, and the intensity scaling. We have also designed targets with wavelength-scale, front-surface structure that greatly enhances various aspects of the laser-target interaction leading to better laser conversion efficiency, higher energy electrons, higher energy protons accelerated by the target normal sheath acceleration mechanism, and, most intriguingly, to compression of the laser spot size for greatly increased peak intensities. We have performed a series of experiments exploring a range of structures including rod and tube shapes and shown significant improvements in energetic electron generation that is reasonably well predicted by PIC simulation. Finally, we have performed experiments pointing the way to the next stages of this research program.

Refereed Publications:

1. L. L. Ji, A. Pukhov, I. Yu. Kostyukov, B. F. Shen, and K. Akli; "Radiation-Reaction Trapping of Electrons in Extreme Laser Fields", **Physical Review Letters 112, 145003 (2014).** DOI: 10.1103/PhysRevLett.112.145003
2. L. L. Ji, A. Pukhov, E. N. Nerush, I. Yu. Kostyukov, B. F. Shen, and K. U. Akli; "Energy partition, gamma ray emission, and radiation reaction in the near-quantum electrodynamics regime of laser-plasma interaction", **Physics of Plasmas 21, 023109 (2014).** DOI: 10.1063/1.4866014
3. L. I. Ji, A. Pukhov, E. N. Nerush, I. Yu. Kostyukov, K. U. Akli, and B. F. Shen, "Near QED regime of laser interaction with overdense plasmas", European Physics Journal of Special Topics 223, 1069-1082 (2014). DOI: 10.1140/epjst/e2014-02158-2
4. L. L. Ji, J. Snyder, A. Pukhov, R. R. Freeman, and K. U. Akli, "Towards manipulating relativistic laser pulses with micro-tube plasma lenses". **Scientific Reports 6, 23256 (2016);** DOI: 10.1038/srep23256
5. S. Jiang, L. L. Ji, H. Audesirk, K. M. George, J. Snyder, A. Krygier, P. Poole, C. Willis, R. Daskalova, E. Chowdhury, N. S. Lewis, D. W. Schumacher, A. Pukhov, R. R. Freeman, and K. U. Akli, "Microengineering laser plasma interactions at relativistic intensities", **Phys. Rev. Lett. 116, 085002 (2016).** DOI: 10.1103/PhysRevLett.116.085002
6. J. Snyder, L. L. Ji, and K. U. Akli, "Enhancement on Laser Intensity and Proton Acceleration Using Micro-tube Plasma Lens Targets" **Phys. Plasmas 23, 123122 (2016).** DOI: 10.1063/1.4972577
7. Liangliang Ji, Sheng Jiang, Alexander Pukhov, Richard Freeman, and Kramer Akli, "Exploring novel target structures for manipulating relativistic laser–plasma interaction," **High Power Laser Science and Engineering 5, e14 (2017).** DOI:10.1017/hpl.2017.12

Submitted for publication:

L. L. Ji, J. Snyder, K. M. George, G. E. Cochran, R. L. Daskalova, A. Handler, T. Rubin, P. L. Poole, C. Willis, E. Chowdhury, B. F. Shen, and D. W. Schumacher, Laser-electron collider within a micro-channel, *submitted to Nature Communications.*

Dissertations and Student Outcomes:

1. J. Snyder, "Leveraging Microscience to Manipulate Laser-Plasma Interactions at Relativistic Intensities," (2016). *Joe has a tenure-track faculty position at Miami University – Hamilton.*
2. K. George, "Modifying the Target Normal Sheath Accelerated Ion Spectrum Using Structured Targets", (2016). *Kevin got a job at Optonicus, a high-tech optics firm in Dayton, OH.*

PROJECT SUMMARY:

(Reference numbers refer to the publication list on page 3.)

Detecting extreme light effects – signatures of the radiation reaction.

One component of this research program has been the identification of extreme light effects in soon-to-be-available experiments. Although the highest intensity yet achieved is ~10^{22} W/cm^2, the highest intensities demonstrated in practical experiments are somewhat lower. However, extension to 10^{23} W/cm^2 is expected soon either via upgrades to existing laser systems (eg. energy enhancements, use of F/1 focusing optics combined with deformable mirrors, etc.) or new systems coming on-line (eg. the Extreme Light Infrastructure pillars). We have identified signatures of radiation-reaction that may be observed with this new capability (see publications 1-3).

Radiation-reaction trapping (RRT) of electrons was revealed in the regime approaching quantum-electro dynamic scales for the laser-plasma interaction. Here electrons quivering in the laser pulse experience the radiation reaction (RR) recoil force by radiating photons. In the following, we will refer to the dimensionless field parameter $a_o = eE_o/m\omega c$, where E and ω are the laser peak electric field magnitude and frequency, e and m are the fundamental charge and mass, and c is the speed of light. For $a_o = 500$ (about $5x10^{23}$ W/cm^2 for 800 nm light), the RR force becomes significant enough to compensate for the expelling laser ponderomotive force. Some electrons are trapped inside the laser pulse instead of being scattered off transversely and form a dense plasma bunch. The mechanism was demonstrated by comparing 3D particle-in-cell (PIC) simulations with and without a RR model employed. Fig. 1 shows results for an $a_o = 500$ laser pulse in a hydrogen plasma with electron number density $n = 20\ n_c$ where n_c is the non-relativistic critical density. In both cases, the initially overdense plasma becomes relativistically transparent, but the relativistic motion of the electrons under RR is sharply modified resulting in a trapping of particles on and near the laser axis. A significant part of the laser energy is then converted into high-energy photons, MeV γ rays, which provide a dramatic signature of the effect (Fig. 1g). Note that the peak laser intensity is strongly reduced (Fig. 1c and 1f). We show that this is a threshold effect and develop a criterion

for significant RRT effects, Fig. 2, namely that as much or more energy goes into the photon channel as into hot electrons ($E\gamma / E_e \geq 1$).

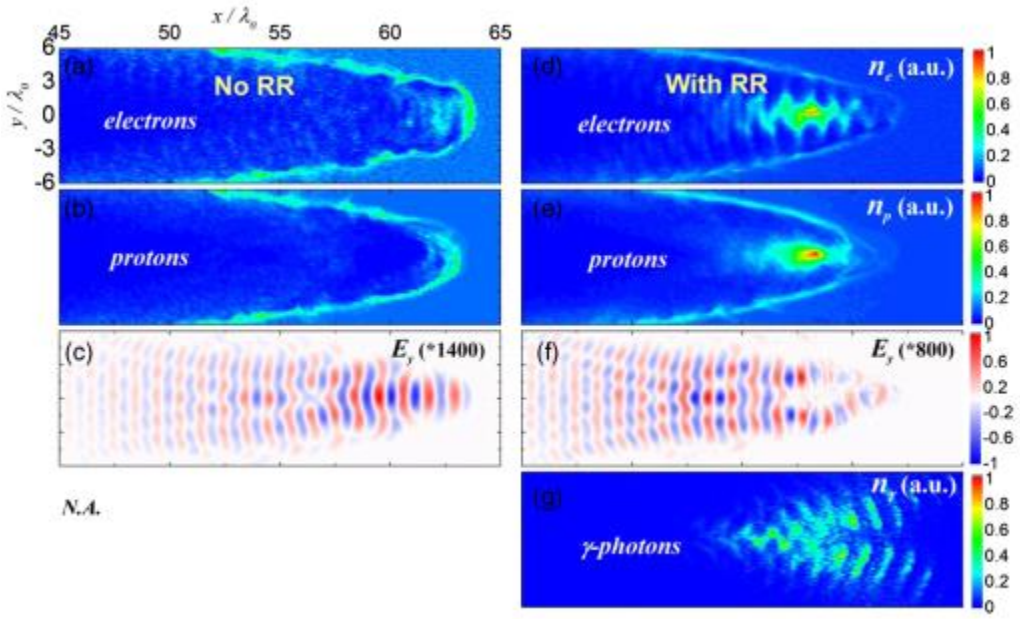

Figure 1. Simulation results of a laser pulse with a_o = 500 in an n = 20 n_c plasma. Distributions of electron and proton densities and the laser field without RR (a-c) and with RR (d-f) modeling. The density distribution of emitted γ photons is shown in (g). (from (1))

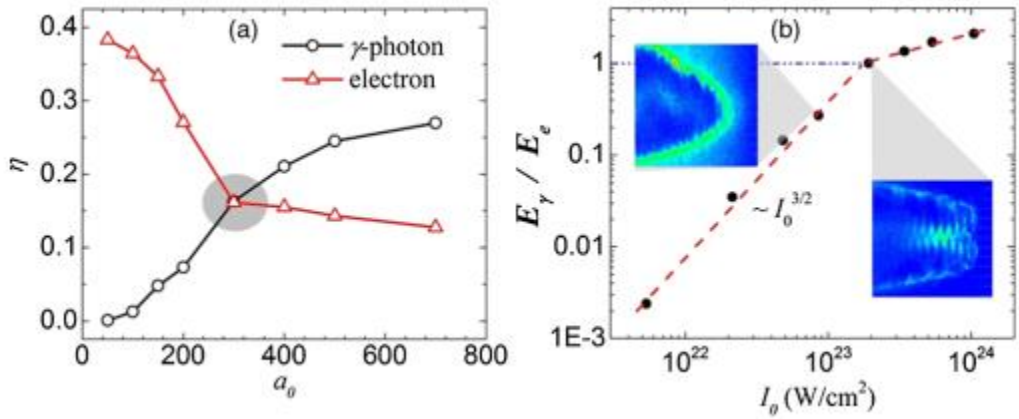

Figure 2. (a) Energy absorbed by electrons and high energy photons (γ) relative to the total laser energy versus the laser field amplitude. (b) The ratio of these energies versus intensity. The insets show the electron density distribution. (from (1))

Structured targets to enhance laser-target coupling and hot electron generation.

We had shown in previous work supported by AFOSR (Jiang, *et al.*, PRE (2014)) that structures with wavelength scale structures on the front (laser-side) surface could enhance laser coupling to energetic electron via two mechanisms: (1) Efficient injection of electrons into the laser pulse followed by direct laser acceleration; and (2) Guiding of the electrons by quasi-static electric and magnetic fields generated as part of the laser-plasma interaction. In this project, we demonstrated these effects experimentally using our laser, Scarlet. Fig. 3 shows a micrograph of the rod-like structures and electron spectra comparing structured and flat targets. The enhancement is clear and dramatic. The results were also reasonably well described in PIC simulations (not shown). These results were described in (5).

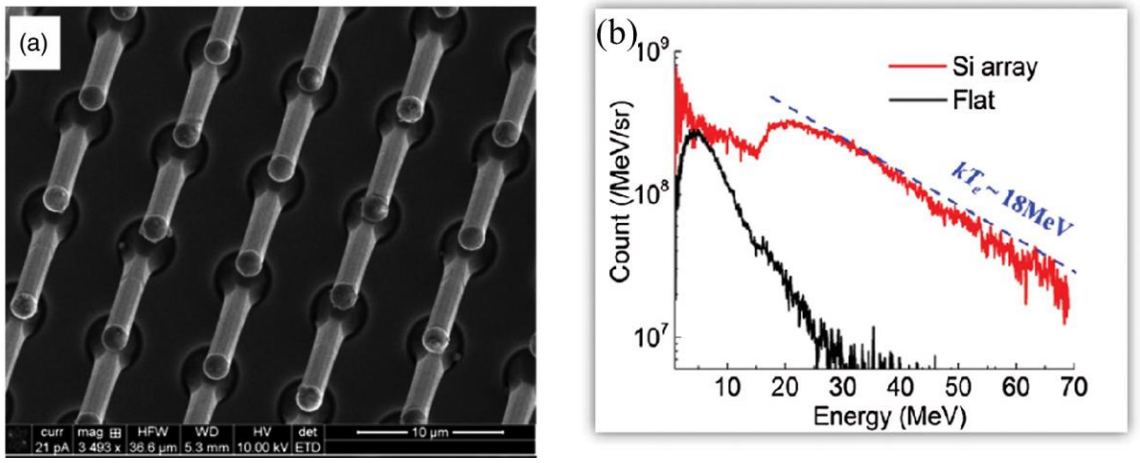

Fig. 3. (a) Micrograph of rod targets (note scale at lower left hard corner) and, (b) electron spectra comparing structured and flat (unstructured) targets. The laser pulses were 30 fs in duration and had a peak intensity near 1 x 10^{21} W/cm^2. The laser was focused in the middle of four rods, although there was significant beam position jitter. (from 5)

Development of structured targets to reach the extreme light regime using current laser capability.

To increase the light intensity, one or a combination of the pulse parameters (energy, duration, and spot size) must be manipulated accordingly. Increasing the energy and/or shortening the pulse require using large optical elements due to damage threshold constraints. Other nonconventional approaches to altering the incident laser pulse such as self-focusing, pulse modification with capillaries, coherent focusing of harmonics, and

flying mirror have been proposed. We have outlined a novel approach that leverages recent advances in micro-engineering of materials and high contrast lasers to boost light intensity using hollow micro-cylinders. We performed a series of 3D PIC simulations to systematically study light intensification in a hollow micro-cylinder with a diameter of 4.8 μm, several times the laser wavelength of 800 nm. We have identified three distinct regimes of intensification: 1) The diffraction regime where the intensification factor is constant at around $\eta \approx 2.6$ for input laser amplitudes below $I_{input} \sim 10^{19}$ Wcm^{-2}); 2) The depletion regime where, in addition to the creation of a diffraction "hot spot", the laser field is depleted by the under-dense plasma electrons, leading to slightly lower intensification factors compared to the ones in the diffraction regime; and 3) The focusing regime where we observe a monotonic increase of the in-tube pulse intensity. This is a strong field effect due to dynamic reshaping of the plasma within the tube and its interaction with the pulse. A laser beam with an initial intensity of $2.4x10^{22}$ Wcm^{-2} could be boosted to a peak intensity of 10^{23} Wcm^{-2} using such a Micro-Tube-Plasma (MTP) lens (see Fig. 4). Such a structure, or perhaps two in tandem, might allow us to reach significantly higher intensities than current facilities are capable of.

By varying the dimensions of the MTP lens, we characterized the in-tube laser pulse to optimize the on-target intensity. We established a potential application of the MTP lens target at current achievable intensities by demonstrating an enhancement in proton energy when comparing to traditional flat interfaces. The enhanced ion acceleration is a result of laser pulse intensification as well as localized electron bunches that are guided by the MTP walls. Other intensity favorable mechanisms such as radiation pressure acceleration (RPA), break-out afterburner acceleration (BOA), and X-ray generation would likely benefit more so than TNSA from the MTP target. Our results show that with current laser and 3D printing technology, it is possible to increase the on-target intensity and efficiently accelerate ions to significantly higher energies.

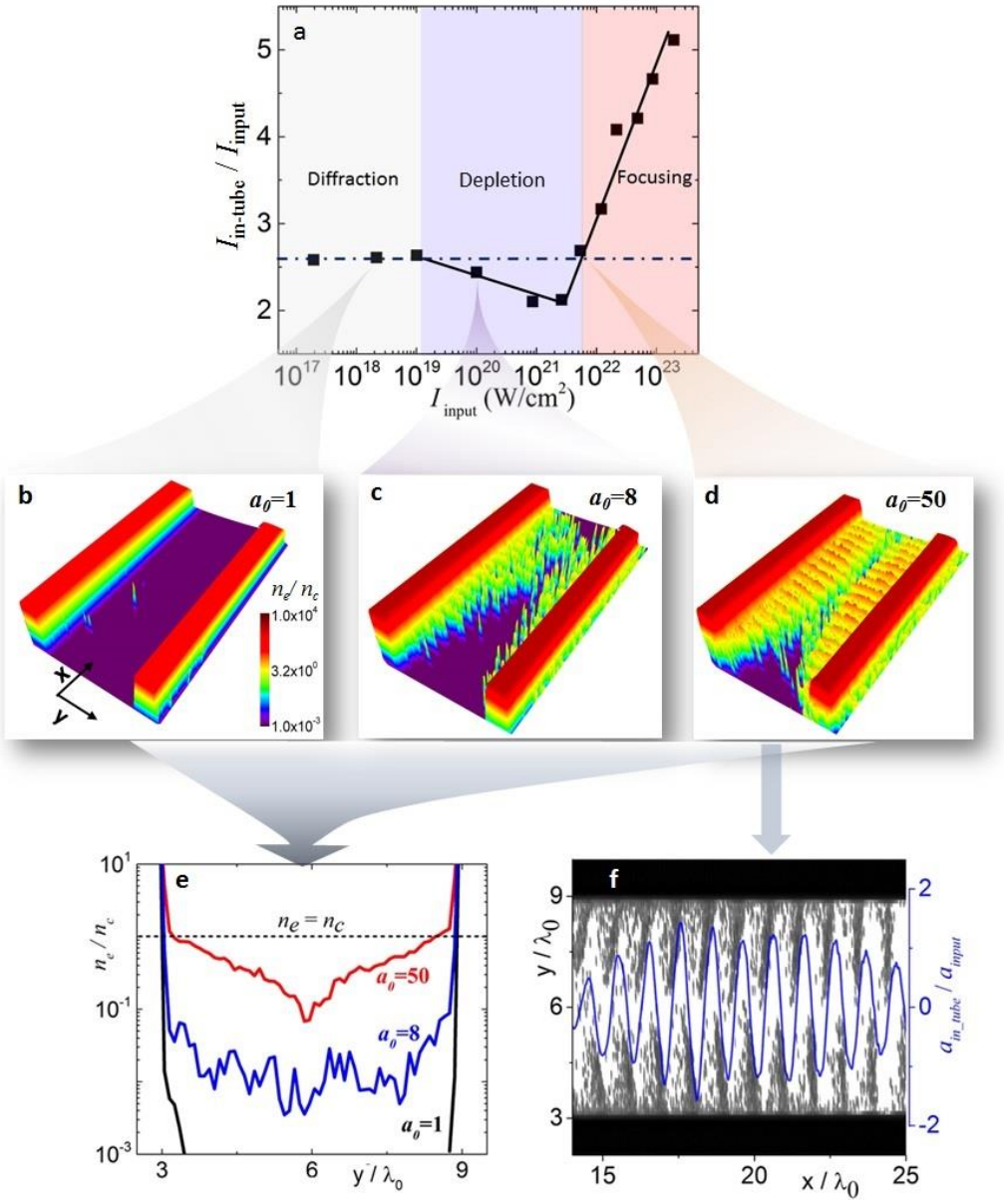

Figure 4. Scaling of light intensification as a function of light intensity. (a) The light intensification factor in three different intensity regions. (b)-(d) Typical electron density distribution in the diffraction, depleting and focusing regions, respectively. (e) Averaged electron density lineouts along the transverse axis *y*. (f) Laser field and electron density in the *x*-*y* plane for a_o = 50. (from (4))

Optimized use of MTPs for ion acceleration.

In work described in (6,7), we looked at using MTPs to accelerate ions using 3D PIC simulations. This was examined in (4), but here we found we could get comparable results using an order of magnitude lower intensity, 5 x 10^{21} W/cm^2, which is within the capability of our laser, Scarlet, and many other lasers now operating. Moreover, we identified a new enhancement mechanism responsible for the increased proton energy and yield predicted by our simulations. A summary of our results is shown in Table 1 and Fig. 5, where the latter plots the proton spectrum from flat foils at two different

intensities (specified in terms of a_o; $a_o = 50 \rightarrow \sim 5x10^{21}$ W/cm^2, $a_o = 87 \rightarrow \sim 2x10^{22}$ W/cm^2) and the results using MTPs of two different diameters. The increase in peak energy is obvious and dramatic.

Case	ID	Length	η_{peak}	η_{ave}	σ (FWHM)	$E_{p,max}(MeV)$
0	-	-	-	-	$3.6\lambda \times 3.6\lambda$	66
1	2λ	1.6λ	8.56	3.2	$0.7\lambda \times 0.8\lambda$	104
2	3λ	2.2λ	7.40	3.44	$0.9\lambda \times 1.0\lambda$	123
3	4λ	4.0λ	8.36	5.0	$0.9\lambda \times 1.0\lambda$	167
4	5λ	5.1λ	5.68	3.44	$1.3\lambda \times 1.4\lambda$	180
5	6λ	8.0λ	4.22	3.1	$1.4\lambda \times 1.5\lambda$	232
6	7λ	10.5λ	2.41	2.15	$1.7\lambda \times 1.9\lambda$	228
7	-	-	3.15	3.24	$1.5\lambda \times 1.5\lambda$	78

TABLE I. Beam characterization within the micro-tube plasma lens. Case 0 details the input pulse, while cases 1-6 show the effects of varying the ID of a micro-tube plasma lens. The length column represents the distance from the entrance of the MTP lens where the peak intensity occurs. The peak intensification is defined as $\eta_{peak} = I_{peak,\,in\,tube}/I_{peak,\,input}$. The average intensification, $\eta_{ave} = I_{ave,\,in\,tube}/I_{ave,\,input}$, is calculated by an averaging technique described in the body of the paper. The spot size is listed as the FWHM in $y \times z$ for the pulse averaged in space over a half wavelength at the time of peak intensity. Case 7 details the characterized pulse with $a_0 = 87$ used to determine the effects of light intensification without the MTP plasma effects included.

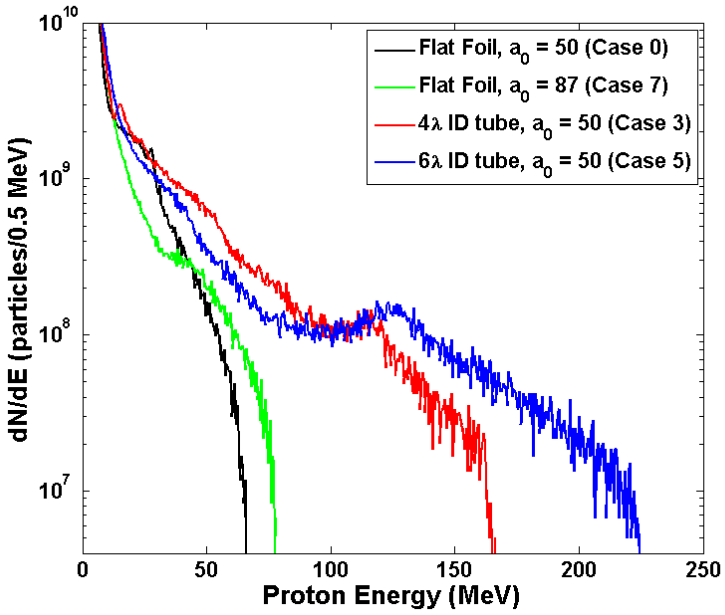

Figure 5. Proton energy distributions for the indicated cases listed in Table 1. (from (6)).

New experimental chamber.

Support from this project and an AFOSR DURIP was used for a major upgrade of the Scarlet experimental chamber. The new chamber is a ¾-scale version of that at the Jupiter Laser Facility. It is four times larger than our previous chamber and has more ports, including 38 large aperture ports and 7 doors for easy access to the interior. Careful analysis of floor loading was required during the design phase and all of our diagnostics had to be reconfigured for use with the new system. Fig. 6 shows photos of the system after it was commissioned. Fig. 7 shows a configuration used for testing and suitable for ion acceleration studies. All Year 3 experiments at OSU for this project were performed using this system.

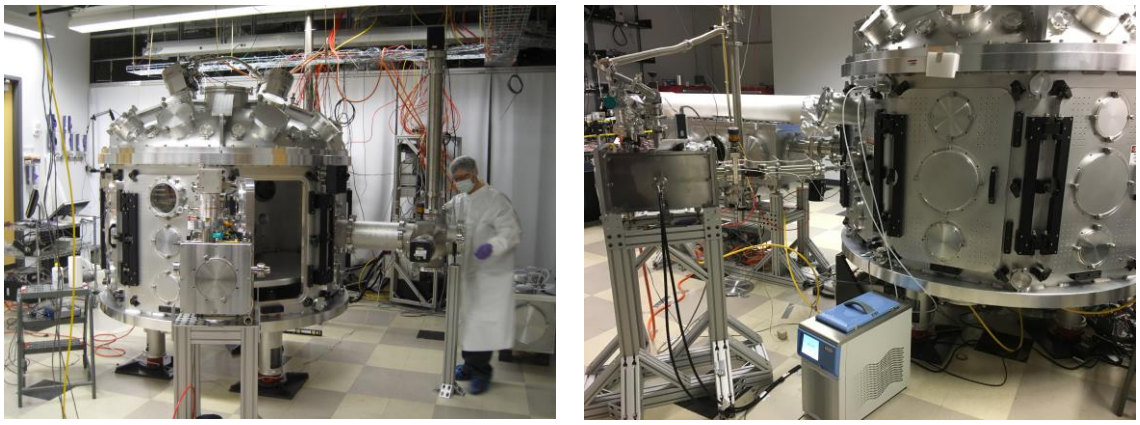

Figure 6. Photos of the new chamber system.

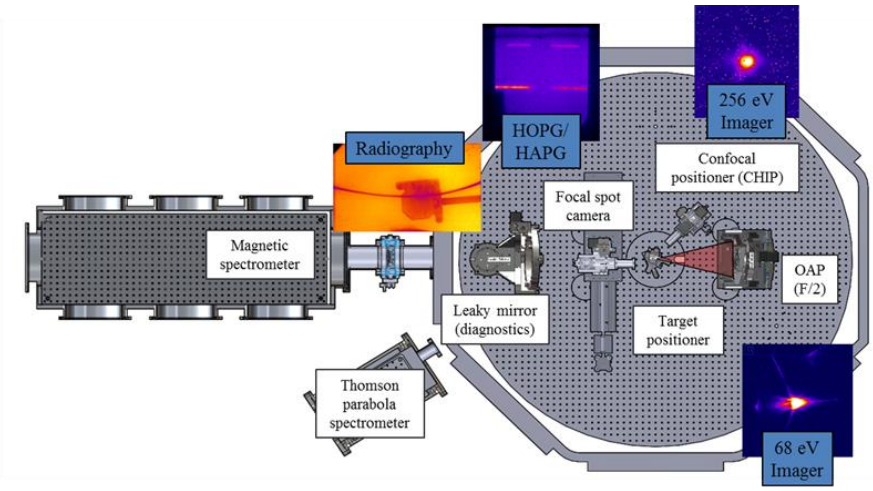

Figure 7. Test configuration and typical layout for an ion acceleration study.

Experimental study of hot electron generation from MTPs

The enhanced ion acceleration seen in Fig. 5 comes from a predicted enhancement in hot electron generation and from the nature of the resulting electron beam, which is predicted to be more collimated and structured in a way that greatly increases the sheath field formed at the back of the target substrate supporting the MTP structures. Accordingly, we decided to start by measuring this hot electron generation. We performed an experiment

using Scarlet at 10^{21} W/cm^2 and incorporating a plasma mirror for contrast enhancement. The results are summarized in Fig. 8. Here we see the results of an MTP compared to a reference target, a 2 μm thick, unstructured copper foil. The MTP was achieved by using sections of a microchannel plate detector. With 5 μm diameter holes and a hole-to-hole spacing of 6 μm, it was convenient and relatively inexpensive. The increase in electron energy and yield is, again, obvious and dramatic. The results are also reasonably well predicted by our PIC simulations. This work has been submitted for publication along with a novel idea for achieving the extreme relativistic regime described next.

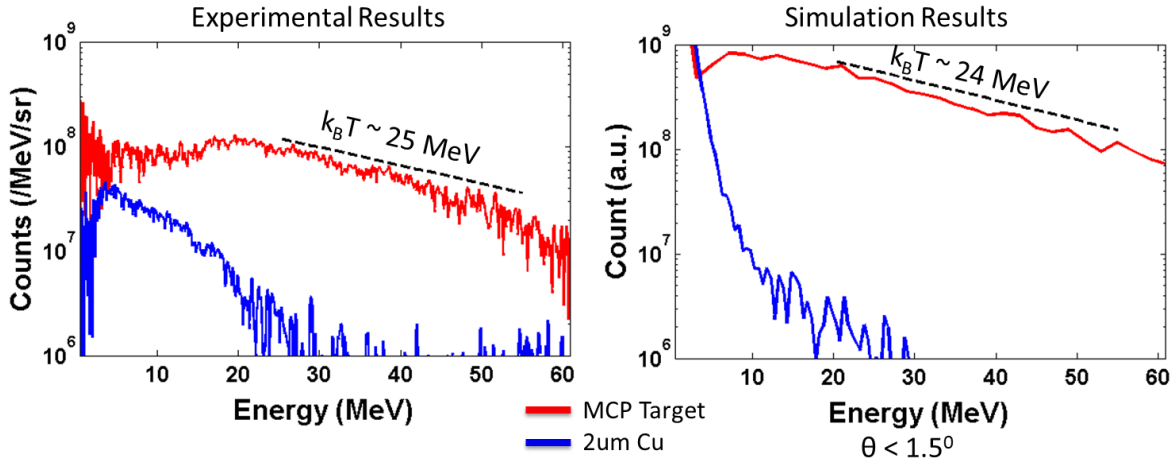

Figure 8. Measured hot electron spectra (left) and prediction from PIC simulations (right). In both cases, the red line is for an MTP and the blue line is for a reference flat (unstructured) copper target. The slope temperature of the hot electrons is indicated using a dashed, black line.

Continuing our collaboration with Ji (now at SIOM), we have proposed a laser-electron collider based on the microchannel-plate target. By placing a well-seated foil on the rear surface of the target, the tube will effectively be closed by a plasma mirror that will redirect the pulse back on itself resulting in a collision between the still-relativistic laser pulse and the highly energetic pulse of electrons excited and accelerated by the pulse on its transit through the tube. This collision could give rise to efficient generation of γ photons in the RR regime using a short pulse laser in the several-petawatt regime. The advantage of a colliding geometry has long been realized, but implementation is difficult. The advantage of this approach is that it is self-aligning. A series of simulations have been performed demonstrating the approach.

This report now concludes with a discussion of the last experiments performed under this project. All experimental work is complete so far as we know, but significant analysis remains to be done and this effort will continue beyond the expiration of this project. We expect new publications to result and these will properly credit the BRI program.

Experimental study using pill box structures.

The pillbox structures were developed in-house and are shown in Fig. 9. Two experiments were performed using Scarlet, the first without a plasma mirror. Based on

these initial results, we decided a plasma mirror was required and ran a second experiment.

The proton beams emerging from the targets were found to be highly structured (Fig. 10) making accurate measurement of the proton spectra unreliable due to the small angular acceptance of our spectrometers. However, we could obtain total dose and rough spectra using radiochromic film packs, and we observed a 55% increase in yield when comparing the best structured target to the best unstructured target consisting of a flat film of photoresist. This analysis is still on-going.

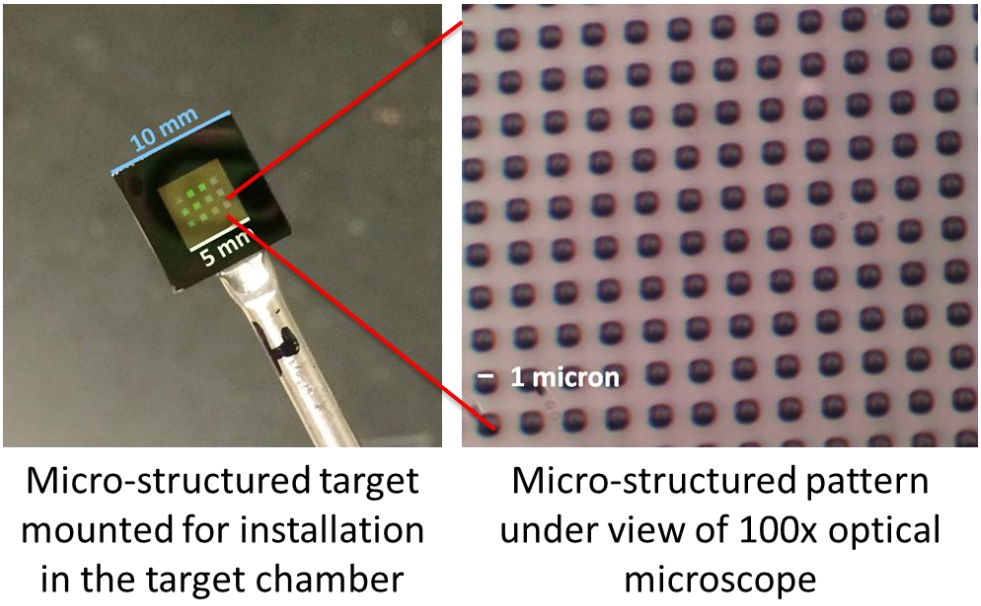

Figure 9. Pillbox structured targets made using optical lithography. Each dot in the mounted target (left) is actually an array of pillboxes, as shown in the optical microscope image (right). The pillboxes are made from photoresist with a 1 μm spacing and width. Two heights were shot: 1 μm and 2 μm.

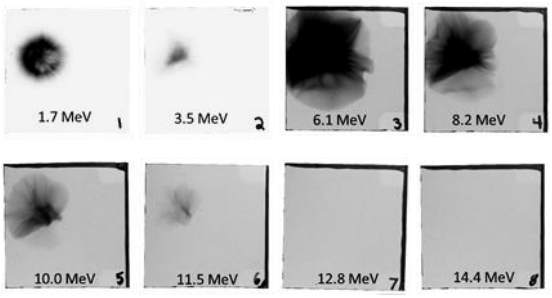

Figure 10. Proton beam spatial profile from a pillbox structure measured using a radiochromic film (RCF) pack. The energy measured by each film layer is indicated in the figure.

Experimental study of liquid crystals films using high energy (>100J) laser pulses.
Two experiments were performed, one using the Texas Petawatt (TPW, University of Texas) and the other using PHELIX (GSI, Darmstadt, Germany). These runs constitute the first time high energy pulses were used with liquid crystal films. We have developed technology that can form high quality, very smooth, reproducible films whose thickness can vary from 10 nm to microns. These films are ideal for ion acceleration studies and might be used in conjunction with the MTP structures. We saw highly energetic protons compared to previous work and performed target thickness scans, taking advantage of the ability of our liquid crystal target insertion technology to tune to the optimum thickness. Fig. 11 describes the experimental geometries used and diagnostics available. Fig. 12 shows some results (but the calibrations are still preliminary). The analysis of this work is on-going.

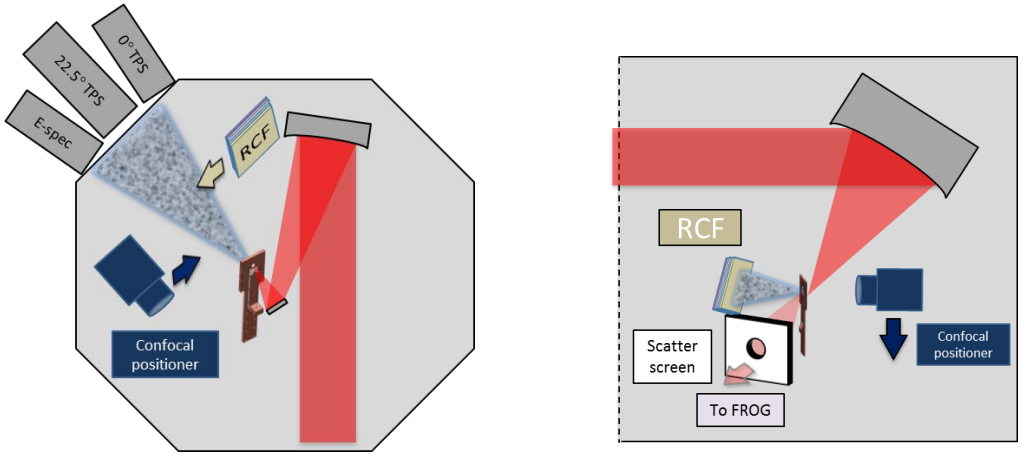

Fig. 11. Ion acceleration experimental setups. Left: Texas Petawatt Laser runs. Right: PHELIX runs. Some Frequency Resolved Optical Gating (FROG) data was collected as well (not shown).

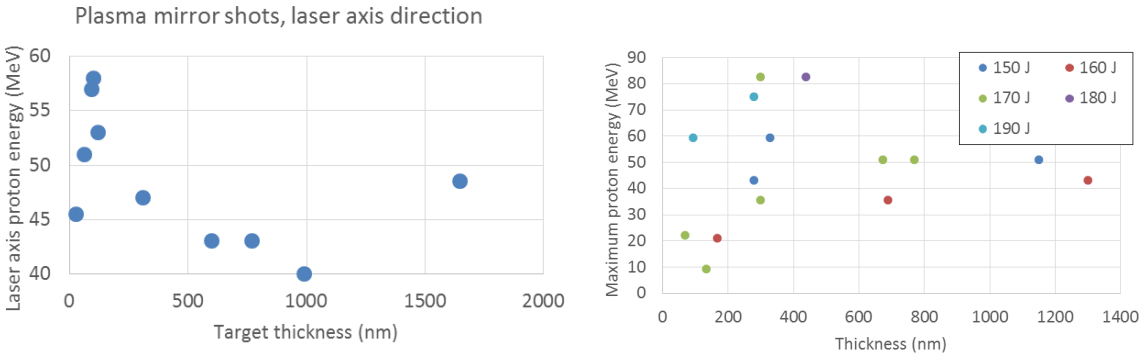

Fig. 12. Ion acceleration results. Left: Results using the Texas Petawatt Laser with energies up to 110 J/pulse and intensities near 10^{21} W/cm^2. The sharp feature for ~100 nm thick targets coincided with features in the proton and carbon spectra. Right: Results using PHELIX. Peak energies exceeding 80 MeV were observed using 100 – 180 J/pulse and intensities up to 10^{20} W/cm^2.